Proceedings of the 10th World Congress on Civil, Structural, and Environmental Engineering (CSEE 2025)
Barcelona, Spain - April, 2025
Paper No. ICSECT 129
DOI: 10.11159/icsect25.129

Creep Effects on an Existing Composite Steel-Concrete Structure

Giada Frappa[1], Margherita Pauletta[1]
[1] Polytechnic Department of Engineering and Architecture, University of Udine,
via delle Scienze 206, Udine 33100, Italy
giada.frappa@uniud.it; margherita.pauletta@uniud.it

Abstract - Steel-concrete composite structures are widely used in modern construction, resulting in highly efficient and robust systems. However, the long-term performance of these structures is significantly affected by concrete creep. This study investigates the long-term effects of concrete creep on the performance of a roof system composed of steel, steel-concrete composite and Reinforced Concrete (RC) elements, in accordance with the Italian Building Code. Using a Finite Element (FE) analysis of the roof, the forces and stresses in the structural members and the displacements of the roof structure are evaluated for the short and long-term conditions. The results show that concrete creep leads to a significant increase in the downward vertical displacement and in the deflection of the composite steel-concrete beams. The study also examines the redistribution of forces due to creep between the structural elements and the corresponding changes in concrete and steel stresses. The results highlight the importance of considering concrete creep in the design and analysis of composite steel-concrete systems to ensure structural safety and serviceability.

***Keywords*:** concrete creep; creep coefficient; long-term effects; composite steel-concrete structures; durability; deflection;

1. Introduction

Steel-concrete composite structures combine the high tensile strength of steel with the compressive strength of concrete to produce highly efficient and robust structural systems. This efficiency results from the complementary interaction between the two materials, each of which has different mechanical properties, such as significantly different Young's moduli. Steel provides high ductility and the ability to resist tensile forces, while concrete excels in resisting compressive stresses, resulting in a synergy that enhances the overall performance of the structure. In composite beams subjected to flexural loads, this pairing achieves exceptional flexural stiffness, making such systems particularly advantageous for narrow spans and long elements.

Due to their superior strength, durability, cost effectiveness and design versatility, steel-concrete composite structures are widely used in a variety of applications. These include bridges requiring robust load-bearing capacity, tall buildings with slender profiles, and industrial plants where durability and efficiency are critical. This combination of materials allows engineers to optimise designs for both functionality and economy [1]-[9].

However, the long-term performance of these structures is significantly affected by the time-dependent behaviour of concrete under sustained loading, known as creep. This phenomenon, which results from the viscoelastic properties of concrete, is characterised by gradual deformation under constant loading [10]. While the steel component is largely unaffected by creep at ambient temperature [11], the deformations induced in the concrete by creep can alter the overall behaviour and performance of the structure. Key effects include stress redistribution between the steel and concrete components, increased deflections, relaxation in shear connections and long-term serviceability issues. These issues are particularly critical in composite beams, where neglecting creep can compromise serviceability, durability, and structural stability. Over time, creep can lead to problems such as excessive deflection, altered load sharing behaviour and a reduction in the effective stiffness of the structure. Therefore, consideration of creep in the design and analysis of composite steel-concrete structures is essential to ensure reliable performance over the life of the structure.

This study investigates the effects of concrete creep on the structural performance of a roof system composed of steel, steel-concrete composite and RC elements, in accordance with the Italian Building Code [12]. The analysis compares the forces and stresses in the main structural elements and the vertical displacements of the roof under both short-term and long-term conditions.

2. Case Study

2.1. Roof Description

The case study considered in this work is the roof of an existing RC building used for sports activities, located in Italy. A view of the FE model of the roof, developed using SAP2000 software [13], is shown in Fig. 1.

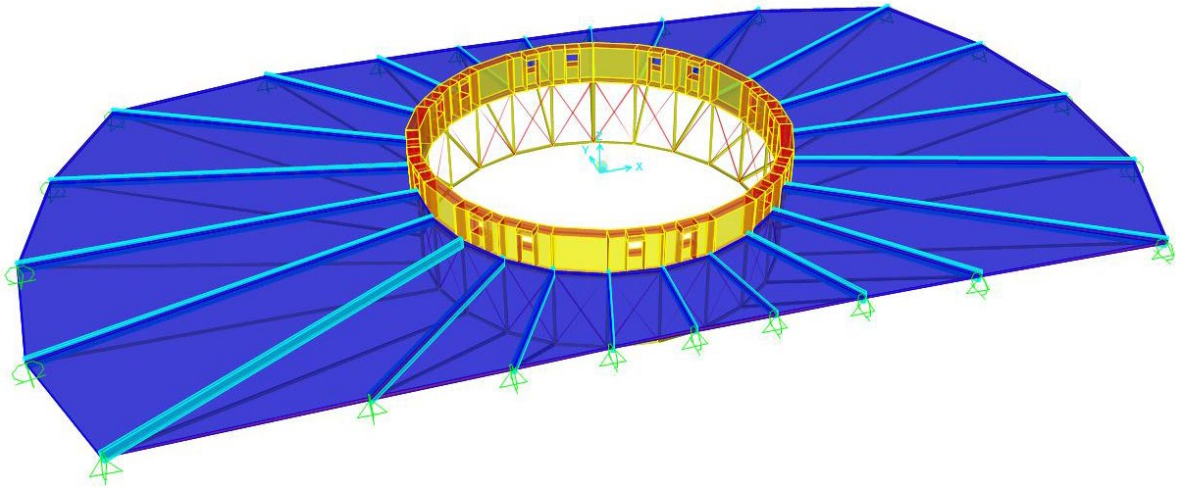

Fig. 1: View of the FE model of the roof.

The roof perimeter consists of two straight parallel sides along the primary direction (X-direction) and two curved arcs in the transverse direction (Y-direction). The dimensions of the roof are approximately 34 m in the X direction and 18 m in the Y direction. Defining the Z axis as parallel to the vertical with positive values pointing upwards, the roof is symmetrical in relation to the Y-Z plane.

The supporting structure of the roof consists of 24 trusses, evenly distributed and positioned radially around the centre of the perimeter to which the curved edges conceptually correspond. Each truss has a triangular static scheme including a top beam, an inclined bottom chord and a vertical strut. The top beam is inclined at 6% from the horizontal plane. The top beam is a steel-concrete composite, consisting of an HEA200 steel section topped by a rectangular RC element of 60x22 cm^2 (Fig. 2). The two components are connected by U-shaped steel connectors welded along the entire length of the upper flange of the steel section. The inclined bottom chord and the vertical strut are made of circular hollow steel sections with a diameter of 9 cm and a wall thickness of 6.5 mm.

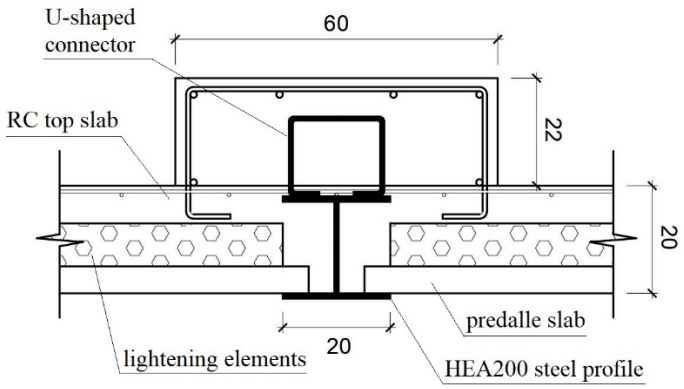

Fig. 2: Structural roof section at the top beam (dimensions are in cm).

Around the perimeter of the building, the radial trusses are supported by RC beams. At the centre of the roof, the node connecting the bottom chord and vertical strut of each truss is connected to the corresponding nodes of adjacent trusses by steel profiles. Together, these profiles form a polygonal truss consisting of 24 steel members lying in a

horizontal plane. These steel members have the same cross-section as the vertical struts and lower chords. The nodes between the upper beams and the vertical struts are connected by a circular RC beam with a rectangular cross-section of 40x140 cm^2 and an internal radius of approximately 5.5 m. This beam has 16 square holes, each with a side length of 50 cm. In addition, diagonal ties made of steel bars 2 cm in diameter connect the nodes between the upper beams and the vertical struts to the lower nodes of the adjacent trusses, forming the polygonal truss.

The roof consists of 24 floor cells, each bounded by the top beams of two adjacent radial trusses, segments of the perimeter beam and portions of the circular RC beam between the respective radial trusses. The floors are constructed from precast predalles slabs, topped with polystyrene lightening elements, and completed with cast-in-place RC beams and a reinforced concrete slab topping (Fig. 3). The predalles slabs are 4 cm thick, 120 cm wide and aligned with their longitudinal axes perpendicular to the bisector of the angle formed by the longitudinal axes of the adjacent radial trusses defining each floor cell. These slabs rest on the bottom flanges of the HEA200 profiles (Fig. 2). The length of each predalles slab varies according to its location and is determined by the average distance between the supporting radial trusses.

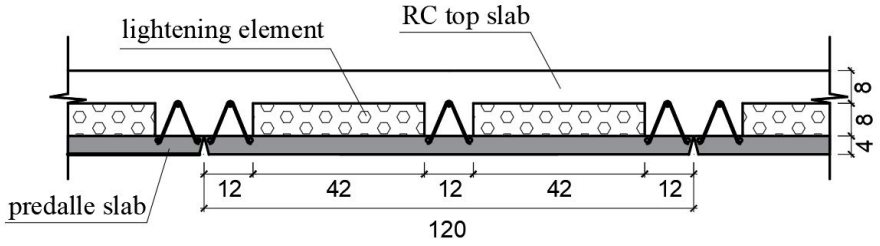

Fig. 3: Floor cross-section.

The beams are 8 cm high and either 12 cm or 24 cm wide, depending on their position: 12 cm when in the middle of a predalles slab and 24 cm when spanning between two successive predalles slabs. The beams are spaced 60 cm apart. The lightening elements in the floor section measure 42x8 cm2.

The RC top slab is covered by the following non-structural layers: a bituminous membrane, 7 cm of XPS insulation, another bituminous membrane, a lightweight concrete screed and a final bituminous membrane.

The top flanges of the HEA200 profiles are fully embedded in the RC slab above the floor, with the transverse reinforcement of the slab extending over these flanges, as shown in Fig. 2. This ensures the continuity of the slab throughout the roof area bounded by the perimeter beams and the circular RC beam.

Due to gaps between adjacent predalles slabs (Fig. 3), these slabs do not make contact along their longitudinal edges. Consequently, the predalles slabs do not contribute to the transmission of compressive or tensile stresses in the direction perpendicular to their longitudinal axes. Therefore, their contribution to the in-plane axial stiffness of the floors in the circumferential direction is negligible.

A 16-sided pyramidal steel frame structure with cellular polycarbonate panels is anchored to the top of the circular RC beam to act as a cover for the central opening.

Gravity loads induce downward vertical displacements in the circular RC beams and radial trusses. Due to the presence of RC beams with finite flexural stiffness under horizontal plane bending along the perimeter of the roof and the radial configuration of the roof support structure, the radial truss ends connected to the perimeter beams undergo horizontal displacements orthogonal to the perimeter beam axis. At the same time, assuming that the perimeter beam is axially inextensible, they impose restraints that prevent the radial truss ends from translating along the axial direction of the perimeter beam. As a result, points at the base of the circular RC beam experience radial horizontal displacements. Specifically, these displacements are outward (away from the centre) for the beam sections connected to shorter radial trusses and inward for those connected to longer radial trusses. At the same time, the ends of the radial trusses connected to the perimeter beams move outwards, perpendicular to the perimeter.

Due to the kinematic behaviour of the load-bearing structure, the floors, because of their in-plane stiffness, interact with the roof load-bearing structure, influencing its deformed shape and thus the forces generated in the structural elements. As a result of this interaction, the floors are subject to in-plane stresses.

2.2. Material Properties

From an experimental testing campaign, the average true cylindrical compressive strength of the concrete was determined to be 42.4 MPa. On the basis of this compressive strength, the average value of the instantaneous modulus of elasticity of the concrete, E_c, was then calculated in accordance with the Italian Building Code [12], giving a value of 33,934 MPa.

The steel sections are of grade Fe430. The average actual yield strength, ultimate strength and Young's modulus of the steel were determined to be 341 MPa, 491.5 MPa and 206,000 MPa respectively.

2.3. Creep Effects

In design practice, creep is considered using the effective modulus method [12]. This method uses a reduced value of the Young's modulus of the concrete, known as the effective modulus, $E_{c,eff}$, which is defined as:

$$E_{c,eff} = \frac{E_c}{1 + \Phi(t, t_0)} \tag{1}$$

where $\Phi(t,t_0)$ is the creep coefficient that characterizes the creep that occurs at time t from the time the load is first applied to the concrete, t_0, after the concrete casting. It is defined as the ratio of the viscous deformation occurring between t_0 and t to the instantaneous elastic deformation in the concrete caused by the applied load. The final amount of creep deformation, i.e. the deformation that occurs as time approaches infinity, is represented by the final creep coefficient, $\Phi(\infty,t_0)$.

In this study, the final amount of creep deformation is considered. The values of $\Phi(\infty,t_0)$ are determined separately for the circular RC beam, top beams and floors according to [12]. These values and the corresponding $E_{c,eff}$ values calculated with Eq. (1) are given in Table 1.

Table 1: Values of $\Phi(\infty,t_0)$ and $E_{c,eff}$ for the circular RC beam, top beams and floors.

	$\Phi(\infty,t_0)$	$E_{c,eff}$ [MPa]
Circular RC beam and Floors	1.70	12.568
Top beams	1.50	13.574

3. Analysis

3.1. FE Model

The FE model of the roof is developed using SAP2000 software (Fig. 1), using frame elements for the 24 radial trusses and the polygonal truss, and two-dimensional shell elements for the circular RC beam.

In order to account for the true in-plane stiffness of the floor cells, the floor cells are modelled by equivalent shell elements that incorporate both plate and membrane behaviour. The in-plane stiffness of the shell in the main directions of the floor is determined using the method proposed in [14].

The effect of the perimeter RC beams on the radial trusses is modelled by assigning restraints to the end trusses supported by the perimeter beams, which prevent translation along the axial direction of the perimeter beams and vertical translations, while allowing translations orthogonal to the perimeter beam axis (Fig. 1).

The analysis considers only the permanent loads due to the self-weight of the roof. The self-weight of the floors, including non-structural elements, is accounted for by applying a distributed load of 4.41 kN/m² to the floor cells. In addition, to account for the weight of the 16-sided pyramidal steel frame structure above the central opening, downward vertical forces of 2.9 kN are applied to the shell elements of the circular beam at the top nodes above the end nodes of the trusses connected to the beam.

To evaluate the forces in the structural elements of the roof and their vertical displacements under two conditions- referred to as the "short-term" condition at the time of load application and the "long-term" condition when the creep deformations have stabilized - two FE models are created. The model representing the "short-term" condition uses the instantaneous Young's modulus of the concrete, E_c, while the model for the "long-term" condition uses the effective moduli, $E_{c,eff}$, shown in Table 1.

In the models, the actual cracked values of flexural and shear stiffness are used for the portions of the circular RC beam that crack under the applied gravity loads. Similarly, for the composite steel-concrete beams that crack under the applied loads, the corresponding cracked values of flexural stiffness are used.

3.2. Type of Analysis

To account for the tendency of the diagonal members to buckle even under very small compressive loads, the frame elements representing the members are modelled to resist only tensile forces. A load-controlled non-linear static analysis is carried out.

4. Results

4.1. Forces in Composite Steel-Concrete Beams

The top beams that experience the greatest stress are two of the longest radial trusses. Comparison of the short and long term conditions shows significant increases in both axial force (N) and bending moment (M) due to creep, together with the corresponding maximum stresses in concrete, σ_c, and steel, σ_s. In the following, the negative sign indicates compressive axial forces and stresses, while the positive sign indicates tensile forces and stresses.

In the short-term condition N=-83 kN and M=211 kNm, which give values of σ_c and σ_s equal to -16.7 MPa and 184.0 MPa, respectively. In the long-term condition N=-122.7 kN and M=271.4 kNm, which induce σ_c=-15.5 MPa and σ_s=271.3 MPa, respectively. It is observed that despite the increase in axial force and bending moment, the long-term stress in the concrete decreases by 7%, while the stress in the steel experiences an increase of 47%.

4.2. Forces in Steel Members

The maximum axial tensile force acting on the inclined bottom chords is 176.6 kN in the short-term condition and 171.2 kN in the long-term condition. Consequently, the tensile stress in the most stressed inclined bottom chord is reduced by 3.1% due to the effects of creep.

The maximum axial compressive force acting on the vertical struts is -123.3 kN in the short-term condition and -141.1 kN in the long-term condition. As a result, the compressive stress in the most stressed vertical strut increases by 14.4% due to the effects of creep.

4.3. Vertical Displacements and Beam Deflections

The maximum downward vertical displacement of the nodes between the top beams and the vertical struts connected by the circular RC beam is 6.4 cm in the short-term condition and 9.4 cm in the long-term condition, resulting in an increase of 47% due to the effects of concrete creep.

An increase in the deflection of the steel-concrete composite beams is also observed. The maximum deflection of the top beam, measured relative to the columns, increases from 5.7 cm in the short-term condition to 7.4 cm in the long-term condition. For the long-term condition, this deflection exceeds the displacement threshold specified in the Italian Code [12] for the quasi-permanent load combination, which is equal to 1/200 of the beam span.

5. Conclusion

The analysis of the considered case study under short and long-term conditions reveals significant effects of creep on the forces, stresses, and displacements in the composite steel-concrete system. The main results are summarized below:

1) The most stressed top beams show a significant increase in axial force and bending moment due to creep effects. Despite the increased loading, the compressive stress in the concrete decreases by 7%, while the stress in the steel increases significantly by 47%, highlighting the redistribution of forces over time.
2) The maximum axial tensile force in the inclined bottom chords decreases by 3.1% in the long-term condition, indicating a slight relaxation of the tensile stress due to creep effects. The decrease in axial tensile force over time is likely to be a result of creep-induced stress redistribution in the structure, as some of the load previously carried by the bottom chords has been redistributed to other structural elements. Conversely, the maximum axial compressive force in the vertical struts increases by 14.4%, resulting in a slight increase in compressive stress.

3) Concrete creep causes a 47% increase in the maximum downward vertical displacement of the nodes between the top beams and vertical struts. This increase is significant as it exacerbates the cracked condition of the circular RC beam at the top.
4) The deflection of the composite steel-concrete beams also increases with time, with the maximum deflection of the top beam exceeding the code limit for the quasi-permanent load combination in the long-term condition.

The results emphasize the critical effect of creep on the long-term performance of composite steel-concrete structures, with significant increases in stresses, displacements and deflections. These results highlight the importance of considering time-dependent effects such as creep in the design and analysis of such systems to ensure structural safety and serviceability.

Acknowledgements

The research was funded by the European Union Next-GenerationEU (PIANO NAZIONALE DI RIPRESA E RESILIENZA (PNRR) – MISSIONE 4 COMPONENTE 2, INVESTIMENTO 1.5 – D.D. 1058 23/06/2022, ECS00000043), within the Interconnected Nord-Est Innovation Ecosystem (iNEST). This manuscript reflects only the authors' views and opinions, neither the European Union nor the European Commission can be considered responsible for them.

References

[1] M. Elchalakani, P. Ayough and B. Yang, *Single Skin and Double Skin Concrete Filled Tubular Structures*. Woodhead Publishing, 2022.
[2] Y. Wang, M. Khan, D. Li, B. Uy, H. Thai and T. Ngo, "A review on long-term behaviour of steel-concrete composite structures," in *Proceedings of civil engineering of the Eurosteel 2023*, Ce/papers, 2023, vol 6, Issue 3-4, pp. 268-275.
[3] A. Sabsabi, O. Baalbaki, A. Masri and H. Ghanem, "A Parametric Study on the Behavior of Arch Composite Beams Prestressed with External Tendons," *Buildings*, vol. 15, 330, 2025.
[4] E. Cosenza and R. Zandonini, "Composite Construction" in *Handbook of Structural Engineering*, W.F. Chen Ed., CRC. Boca Raton, Florida, 1997, pp. 1-122.
[5] D. Dujmović, C. B. Androić and I. Lukačević, *Composite Structures according to Eurocode 4: Worked Examples*. Berlin, Wilhelm Ernst & Sohn, 2015.
[6] R. P. Johnson, *Composite Structures of Steel and Concrete.* Oxford, Blackwell Publishing, 2004.
[7] D. Oehlers and M. Bradford, *Elementary behavior of composite steel and concrete stuctural members.* Oxford, Butterworth-Heinemann, 1999.
[8] I. Vayas and A. Iliopoulos, *Design of Steel-Concrete Composite Bridge to Eurocodes*. Boca Raton, Florida, CRC Press, Taylor&Francis Group, 2014.
[9] C. Y. Wang, *Steel and Composite Structures, Behavior and Design for Fire Safety*. London, Taylor and Francis Group, 2002.
[10] G. Pons and J. M. Torrenti, "Le retrait et le fluage" in *La durabilité des Bétons*, Presses de l'ENPC, Paris, 2008, pp. 25-27.
[11] C. Constantin, *Calcul de structures de constructions réalisées avec des matériaux à propriétés rhéologiques*. Paris, Edition Hermes, Lavoisier, 2006.
[12] Ministero delle Infrastrutture e dei Trasporti, D.M. 17/01/2018, *Aggiornamento delle «Norme tecniche per le costruzioni»*. Rome.
[13] Computers & Structures, *CSI Analysis Reference Manual, SAP2000®, ETABS®, SAFE®, e CSi-Bridge®*. Berkeley, 2018.
[14] G. Frappa, I. Pitacco, S. Baldassi and M. Pauletta, "Methods to Reproduce In-Plane Deformability of Orthotropic Floors in the Finite Element Models of Buildings," *Appl. Sci*., vol. 13, no. 11, 6733, 2023.